JCI The Journal of Clinical Investigation

Tumor emergence is sensed by self-specific CD44^{hi} memory Tregs that create a dominant tolerogenic environment for tumors in mice

Guillaume Darrasse-Jèze, … , Katrina Podsypanina, David Klatzmann

J Clin Invest. 2009;119(9):2648-2662. https://doi.org/10.1172/JCI36628.

Research Article **Immunology**

Early responses of Tregs and effector T cells (Teffs) to their first encounter with tumor cells have been poorly characterized. Here we have shown, in both implanted and in situ–induced mouse tumor models, that the appearance of tumor cells is immediately sensed by CD44^{hi} memory Tregs that are specific for self antigens. The rapid response of these Tregs preceded and prevented activation of naive antitumor Teffs. The relative speed of the Treg versus the Teff response within the first 2–4 days determined the outcome of the antitumor immune response: tolerance or rejection. If antitumor memory Teffs were present at the time of tumor emergence, both Tregs and Teffs were recruited and activated with memory kinetics; however, the Tregs were unable to control the Teffs, which eradicated the tumor cells. This balance between effector and regulatory responses did not depend on the number of Tregs and Teffs, but rather on their memory status. Thus, in the natural setting, dominant tolerogenic immunosurveillance by self-specific memory Tregs protects tumors, just as it protects normal tissues. More generally, our results reveal that the timing of Treg and Teff engagement, determined by their memory status, is an important mode of regulation of immune responses.

Tumor emergence is sensed by self-specific CD44^{hi} memory Tregs that create a dominant tolerogenic environment for tumors in mice

Guillaume Darrasse-Jèze,[1,2,3] Anne-Sophie Bergot,[1,2,3] Aurélie Durgeau,[1,2,3] Fabienne Billiard,[1,2,3] Benoît L. Salomon,[1,2,3] José L. Cohen,[1,2,3] Bertrand Bellier,[1,2,3] Katrina Podsypanina,[4] and David Klatzmann[1,2,3,5]

[1]UPMC Univ Paris 06, UMR 7211, Immunology-Immunopathology-Immunotherapy (I3), Paris, France. [2]CNRS, UMR 7211, Immunology-Immunopathology-Immunotherapy (I3), Paris, France. [3]INSERM, UMR_S 959, Immunology-Immunopathology-Immunotherapy (I3), Paris, France. [4]Program in Cancer Biology and Genetics, Memorial Sloan-Kettering Cancer Center, New York, New York, USA. [5]AP-HP, Hôpital Pitié-Salpêtrière, Biotherapy, Paris, France.

Early responses of Tregs and effector T cells (Teffs) to their first encounter with tumor cells have been poorly characterized. Here we have shown, in both implanted and in situ–induced mouse tumor models, that the appearance of tumor cells is immediately sensed by CD44^{hi} memory Tregs that are specific for self antigens. The rapid response of these Tregs preceded and prevented activation of naive antitumor Teffs. The relative speed of the Treg versus the Teff response within the first 2–4 days determined the outcome of the antitumor immune response: tolerance or rejection. If antitumor memory Teffs were present at the time of tumor emergence, both Tregs and Teffs were recruited and activated with memory kinetics; however, the Tregs were unable to control the Teffs, which eradicated the tumor cells. This balance between effector and regulatory responses did not depend on the number of Tregs and Teffs, but rather on their memory status. Thus, in the natural setting, dominant tolerogenic immunosurveillance by self-specific memory Tregs protects tumors, just as it protects normal tissues. More generally, our results reveal that the timing of Treg and Teff engagement, determined by their memory status, is an important mode of regulation of immune responses.

Introduction

Beyond immune ignorance (1) or immune surveillance (2), tumors appear to induce immune tolerance (3). There is considerable evidence that tumor immunity (i.e., protection from the immune system) is established by the induction of an active immune tolerance largely mediated by natural Tregs (4–10).

These CD4$^+$ cells are identified by their expression of CD25 and of the Forkhead/winged-helix protein 3 (Foxp3) transcription factor (11, 12). Once activated through their TCR, they suppress immune responses by combinations of several mechanisms (13, 14). The main function of Tregs is thought to be the maintenance of self tolerance, and likewise the control of autoimmune diseases (15). They are also implicated in regulation of various, if not all, immune responses, such as immune responses to infectious agents (16), allergens (17), and alloantigens (18).

Several lines of evidence accumulated since the 1980s suggest that suppressor T cells (19) or Tregs (4, 20) play a major role during immune responses to tumors. In mice or humans, tumor-draining LNs (dLNs) and the tumor itself become infiltrated with Tregs (6, 10, 21, 22), and this abundance is inversely correlated with survival (6). Numerous studies have reported an increase of Tregs in patients with malignancies (20). In many mouse tumor models, CD25$^+$ cell ablation before tumor implantation leads to antigen-specific T cell–mediated tumor eradication (22–25), and the first Treg depletion in cancer patients has been shown to enhance vaccine-induced antitumor immune responses (26). However, despite the numerous observations highlighting the role of Tregs during tumor development, surprisingly little is known concerning the role of Tregs at the very time of cancer emergence. In fact, tumor-triggered immune responses — whether effector or regulatory — are rarely analyzed before day 6–9, at such time when the tumor becomes visible. Moreover, it is not clear whether Treg response is nonspecifically induced by the tumor environment (27) or is specifically triggered by tumor antigens. While some authors proposed that self-specific Tregs can suppress antitumor responses (28, 29), others suggested that Tregs specific for tumor neoantigens are responsible for the induction of tolerance to the tumor (30–32).

As tumor cells express mostly normal self antigens, we reasoned that memory regulatory response to these antigens could be triggered at tumor emergence. Indeed, we previously showed that while some Tregs remain quiescent and have a long lifespan, a subset of memory-like self-specific CD44^{hi} Tregs is constantly activated at the steady state (33). Several lines of evidence indicate that these antigen-experienced activated/memory Tregs (amTregs) are involved in the permanent suppression of immune responses against self antigens (33–35). Their physiological role was recently highlighted by demonstration that Foxp3$^+$ Treg ablation at any time throughout life results in the rapid occurrence of autoimmune diseases (36). We thus hypothesized that amTregs could specifically mediate induction of tolerance to the emerging self-tumors.

In this work, to our knowledge the first report that addresses Treg and effector T cell (Teff) responses at the very time of tumor emergence, we found that self-specific amTregs were

Authorship note: Guillaume Darrasse-Jèze and Anne-Sophie Bergot contributed equally to this work.

Conflict of interest: The authors have declared that no conflict of interest exists.

Citation for this article: *J. Clin. Invest.* **119**:2648–2662 (2009). doi:10.1172/JCI36628.

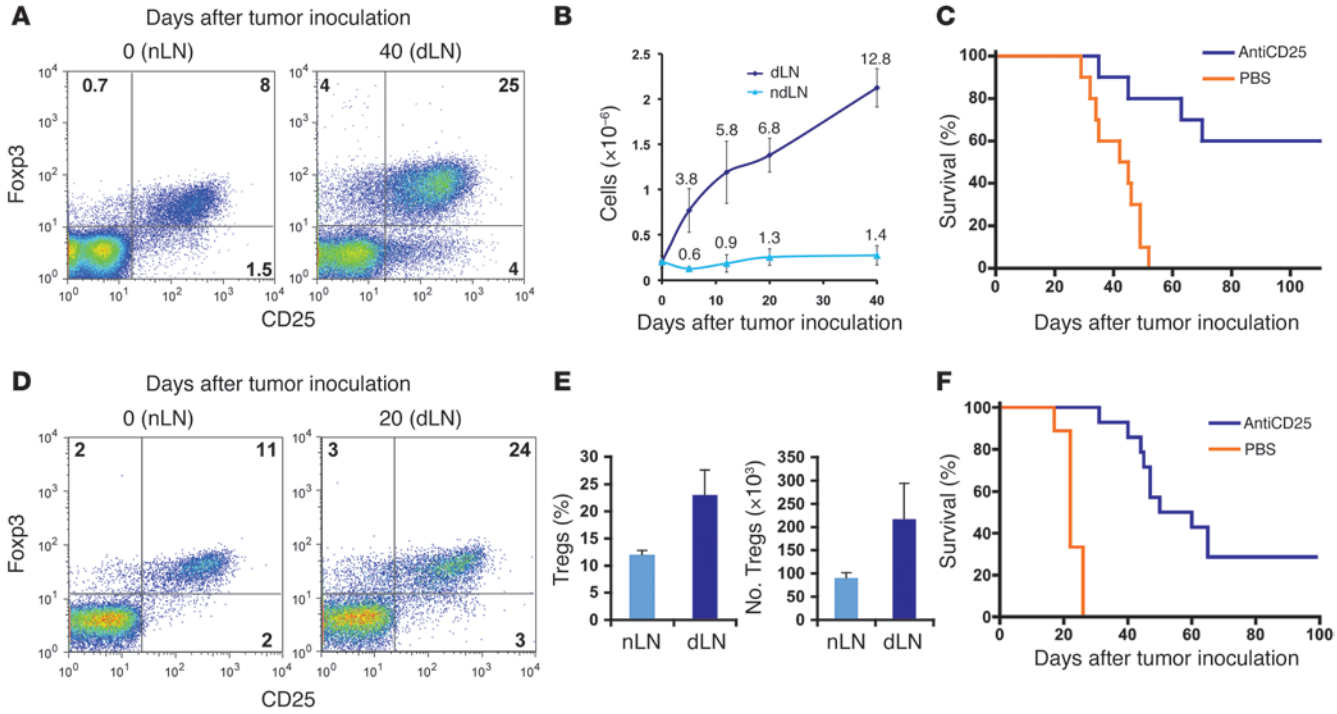

Figure 1

Tumor emergence favors a Treg response that blocks efficient antitumor immune responses. (**A**, **B**, **D**, and **E**) CD4+ gated T cells were analyzed for CD25 and Foxp3 expression by flow cytometry. Control nLNs were taken from normal mice. dLNs and ndLNs of tumor-bearing mice were obtained at the indicated times after s.c. inoculation of 10^5 4T1 tumor cells in BALB/c mice (**A** and **B**) or B16F10 tumor cells in C57BL/6 mice (**D** and **E**). (**A** and **D**) CD25 and Foxp3 flow cytometry profiles of CD4+ T cells. Numbers indicate percentage of cells in the respective quadrants. (**B**) Absolute number of Tregs in 4T1-inoculated dLNs versus ndLNs at indicated times ($P < 0.001$). Fold increases compared with nLNs are indicated above each time point (3 mice per time point). (**E**) Mean percentage of CD4+CD25+Foxp3+ Tregs within CD4+ T cells, and absolute number of Tregs, in B16F10-inoculated dLNs versus nLNs at day 20 ($P < 0.001$). (**C** and **F**) Effect of Treg depletion on tumor growth. BALB/c (**C**) and C57BL/6 mice (**F**) were depleted of Tregs by anti-CD25 Ab treatment and challenged 5 days later with 10^5 4T1 or 2 days later with 10^5 B16F10 tumor cells, respectively. Kaplan-Meyer survival rate was significantly higher (**C**, $P = 0.02$; **F**, $P < 0.001$) in the anti-CD25–treated ($n = 8$ [**C**]; 14 [**F**]) than in the PBS-treated group ($n = 5$ [**C**]; 9 [**F**]). For each model, 1 representative of 5 independent experiments is shown.

activated early and briskly by self antigens expressed by tumors; they overpowered Teffs because they drove a secondary-type immune response against tumor self antigens, by essence more rapid and efficient (37) than the primary-type response of naive Teffs specific for tumor neoantigens. In contrast, the presence of antitumor amTeffs was able to bypass the tumor immunity mediated by self-specific memory Tregs. We show here that prior activation status, and thus pace of activation of self-specific amTregs and tumor-specific Teffs at tumor emergence, dictates the immune response outcome and can be modulated for therapeutic intervention.

Results

Tregs and antitumor Teffs coexist at tumor emergence. We first analyzed the dynamics of Tregs in dLNs of tumor-bearing mice. In BALB/c mice implanted with 4T1 mammary tumor cells, we observed a rapid and continuous increase in both proportion and total number of Foxp3+ T cells in dLNs (Figure 1, A and B). While in normal LNs of tumor-free mice (nLNs), Foxp3+ T cells represented approximately 9% of CD4+ T cells before tumor implantation, their proportion progressively increased to greater than 20%–30% at day 40 after tumor implantation. Since the total number of T cells increased concomitantly in dLNs, this translated as a 13-fold increase in the absolute number of Tregs at day 40. In contrast, the absolute number of Tregs remained stable in the nondraining LNs (ndLNs; Figure 1B). Similar results were obtained with C57BL/6 mice implanted with B16F10 melanoma cells (Figure 1, D and E).

This Treg recruitment contributed to tumor outcome, as Treg ablation by injection of an anti-CD25 mAb just before tumor challenge led to the development of efficient antitumor responses. While tumors continuously grew in control mice, they grew more slowly or even regressed after 8–12 days in Treg-depleted mice (data not shown), resulting in tumor eradication in approximately 50%–60% of the animals for the 4T1 tumors (Figure 1C). Moreover, cured mice spontaneously rejected a second tumor challenge, demonstrating that they had developed an efficient antitumor memory response (data not shown). We obtained similar results in numerous independent experiments using 4T1 or AB1 tumors in BALB/c mice as well as B16F10 tumors in C57BL/6 mice (Figure 1F). Together, these results indicate that Tregs and antitumor Teffs coexist at tumor emergence. It is thus striking that Tregs always overpower Teffs, as demonstrated by tumor growth in the absence of Treg elimination.

Tregs outrun Teffs at tumor implantation. To study the respective activation kinetics of Tregs and other T cells after tumor implantation, we first analyzed the division of ex vivo CFSE-labeled Thy1.1+ T cells obtained from naive mice, injected into 1-day B16F10 tumor–

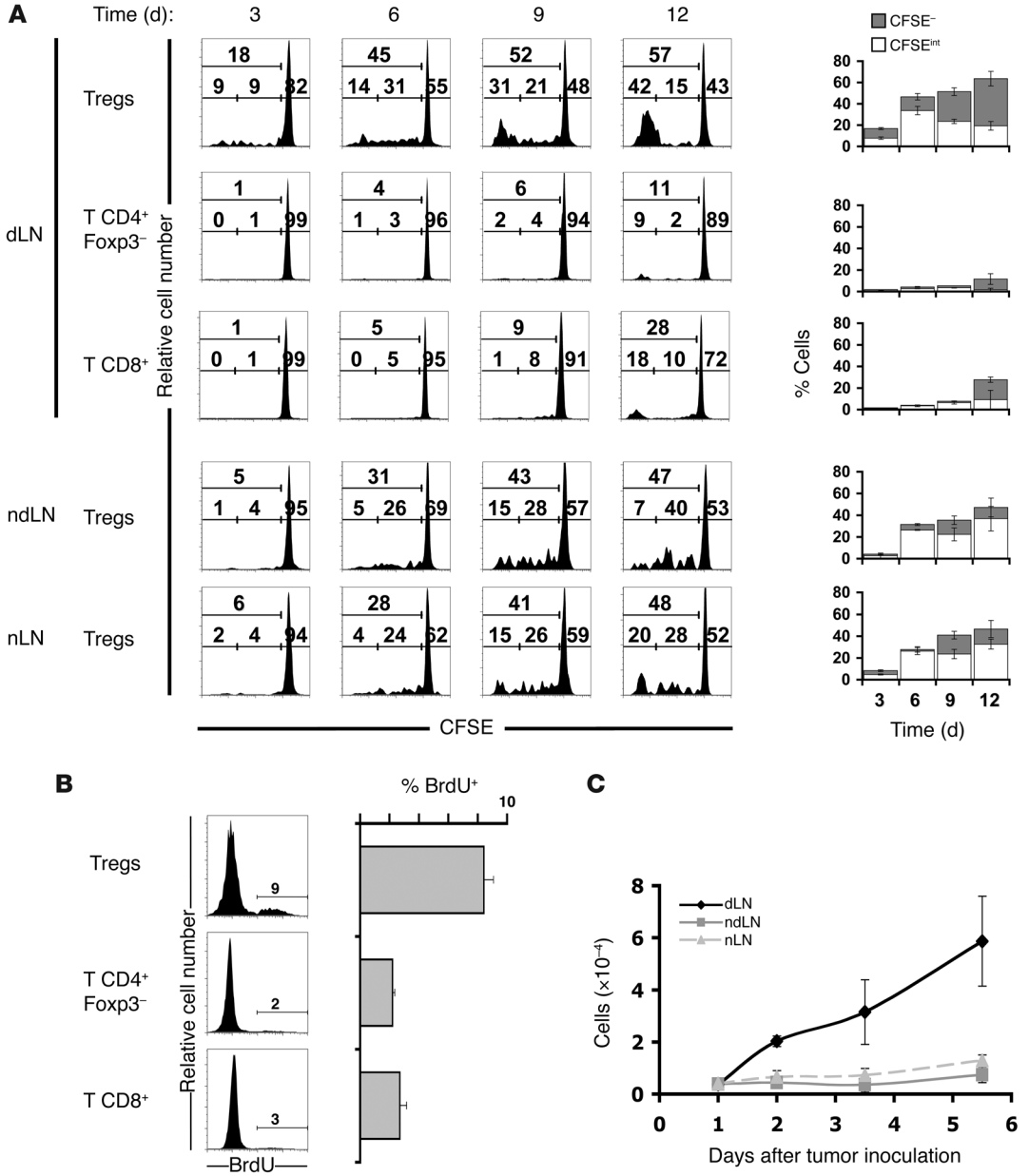

Figure 2

Rapid and intense memory-like proliferation of Tregs at tumor emergence. (**A**) Both 1-day B16F10 tumor-bearing and unmanipulated mice received CFSE-labeled Thy1.1 congenic cells from normal mice. Division profiles of Thy1.1+ donor cells were evaluated by flow cytometry at the indicated times in dLNs, ndLNs, or nLNs. Percentage of cells that had undergone no ($CFSE^{hi}$), few ($CFSE^{int}$), or more than 6 divisions ($CFSE^{–}$), are shown in histograms; the $CFSE^{int}$ and $CFSE^{–}$ percentages are also shown graphically. $CD4^+Foxp3^+$ T cells from dLNs divided significantly more than did other cells ($P < 0.05$). Each panel is representative of 3 mice per experiment (2 independent experiments). (**B**) BrdU incorporation in Tregs and $CD4^+$ and $CD8^+$ T cells from dLNs of tumor-bearing mice on day 2 after 4T1 cell injection, with corresponding percentages of $BrdU^+$ cycling T cells shown graphically. Numbers within histograms denote percentage of cells that incorporated BrdU. Incorporation of BrdU by Tregs was significantly different from that of other T cells ($P < 0.001$; 3 mice per group; 4 independent experiments). (**C**) Increase in absolute number of $BrdU^+$ Tregs in dLNs ($P \leq 0.002$ versus ndLNs and nLNs) of continuously BrdU-treated mice ($n = 3$).

bearing Thy1.2 C57BL/6 mice (Figure 2A). In the dLNs, 3 days after transfer, 18% of the Tregs had already undergone several divisions, while almost no division was detected in the $CD4^+Foxp3^–$ or $CD8^+$ T cells. At day 6, 45% of the Tregs have undergone at least 1 division, and 14% more than 6 divisions. In contrast, modest division of other T cells became detectable in dLNs only at days 9–12. In ndLNs and nLNs, there was substantial division of Tregs, which illustrates the high turnover of the self-reactive Treg subset (33). These divisions were delayed compared with those in dLNs: at day 3, while 9% of the dLN Tregs had divided more than 6 times, 1% had divided in the ndLNs (Figure 2A). Similar results were obtained in 5 independent experiments in which we detected substantial Treg

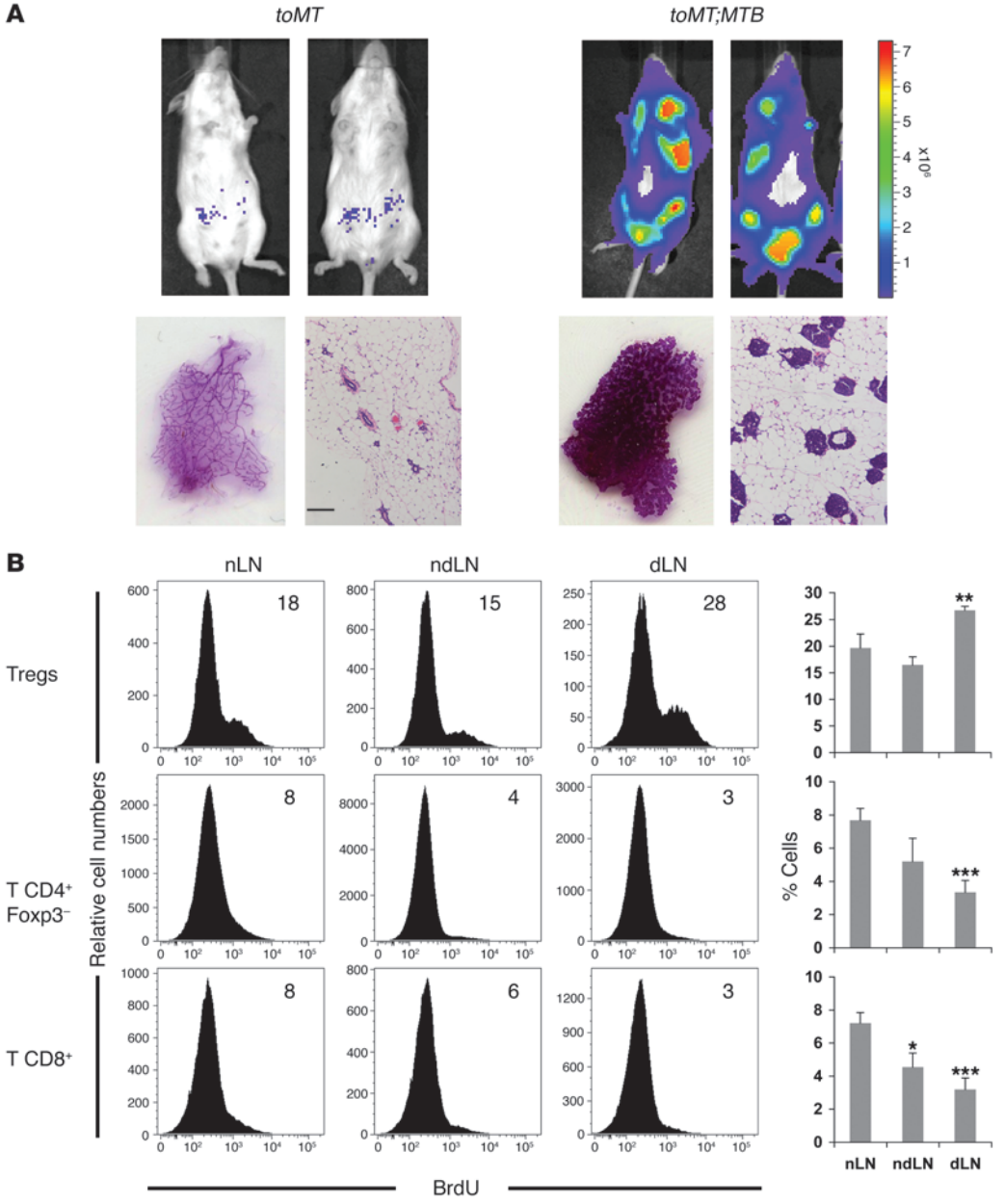

Figure 3

T cell response in mice developing mammary tumors after doxycycline-mediated induction of oncogenes. (**A**) Transgene-expressing cells were analyzed by bioluminescence imaging of the *ToMT:IRES:Luc;MTB* mice, or control mice lacking the *MTB* transgene, given doxycycline and BrdU. Representative images show the presence of signal-emitting cells in the mammary gland areas of bitransgenic mice at day 3 of treatment. Representative whole-mount and H&E stainings of mammary glands of the corresponding mice at day 7 after induction demonstrate widespread mammary tumor development in *ToMT:IRES:Luc;MTB* mice, but not control mice. Scale bar: 100 μm. (**B**) BrdU incorporation in $CD4^+CD25^+Foxp3^+$ Tregs and $CD4^+CD25^-Foxp3^-$ and $CD8^+$ T cells from dLNs and ndLNs of *ToMT:IRES:Luc;MTB* and nLNs of *ToMT:IRES:Luc* control mice. Numbers within histograms indicate the percentage of cells that incorporated BrdU. $n = 4$ (dLN), 2 (ndLN), 6 (nLN). Corresponding percentages of $BrdU^+$ cycling T cells are shown graphically. $^*P < 0.05$, $^{**}P < 0.01$, $^{***}P < 0.005$ versus nLN.

division in dLNs as soon as 1.5–2 days after their injection (data not shown). This phenomenon was also observed in 4T1 tumor–bearing BALB/c mice (Supplemental Figure 1; supplemental material available online with this article; doi:10.1172/JCI36628DS1).

We also analyzed the turnover of T cells in tumor-bearing mice by direct administration of BrdU, a nucleoside analog that is selectively incorporated in the DNA of dividing cells. This method does not require cell transfer and allows for measure of the cumulative absolute number of dividing cells within the natural T cell pool. At day 2 after tumor challenge, BrdU was preferentially incorporated by Tregs (Figure 2B). At day 6, we observed a 6-fold increase in the absolute number of $BrdU^+$ Tregs in dLNs compared with ndLNs or nLNs (Figure 2C). Finally, we also evaluated Treg and Teff activation by analyzing expression of the early activation marker CD69

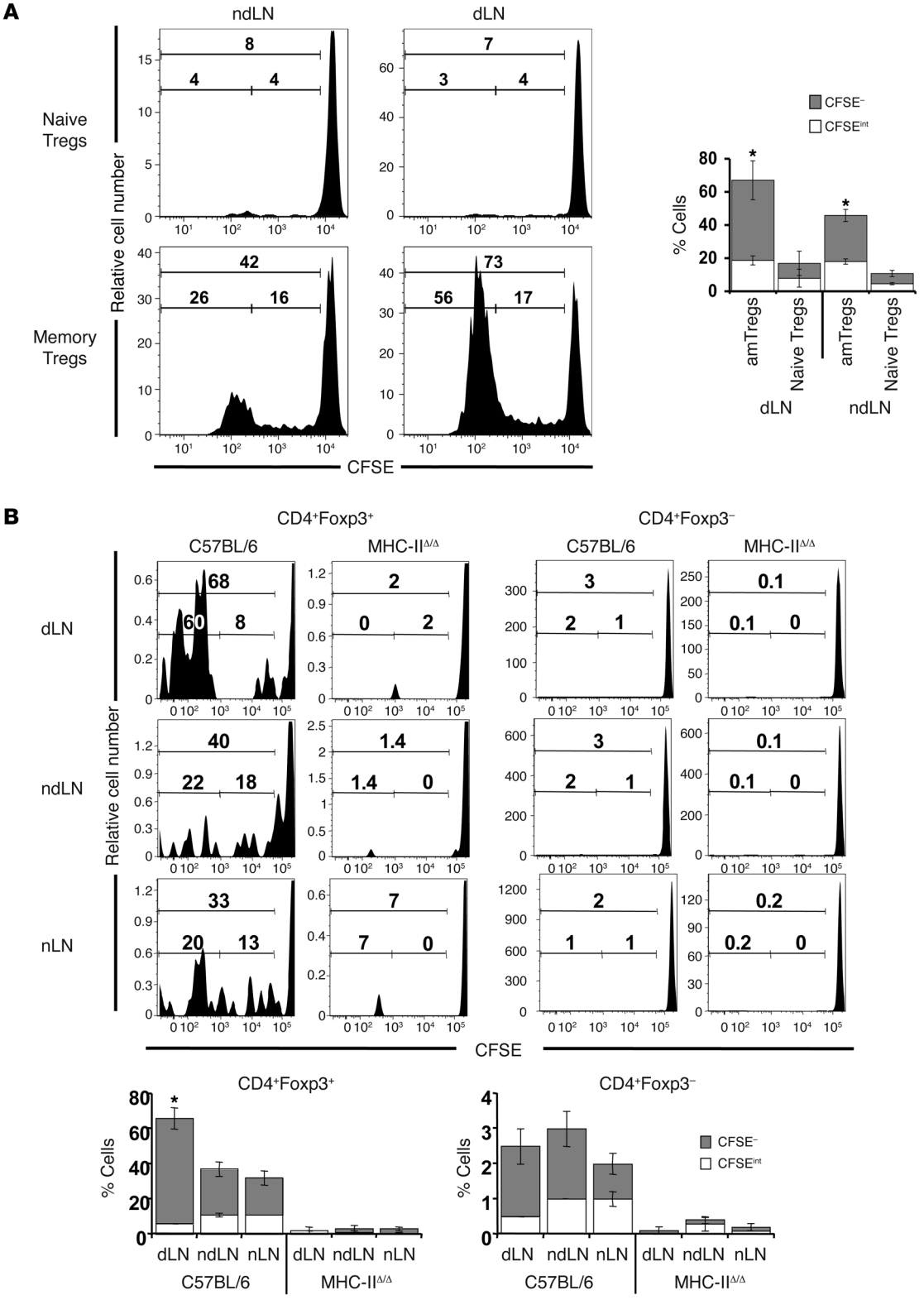
A
ndLN
dLN
Naive Tregs
Memory Tregs
Relative cell number
CFSE
8
4
4
7
3
4
42
26
16
73
56
17
CFSE⁻
CFSEint
% Cells
amTregs
Naive Tregs
dLN
ndLN
B
CD4+Foxp3+
CD4+Foxp3−
C57BL/6
MHC-IIΔ/Δ
dLN
ndLN
nLN
68
60
8
2
0
2
3
2
1
0.1
0.1
0
40
22
18
1.4
1.4
0
3
2
1
0.1
0.1
0
33
20
13
7
7
0
2
1
1
0.2
0.2
0
CFSE
% Cells
dLN ndLN nLN dLN ndLN nLN
C57BL/6
MHC-IIΔ/Δ

Figure 4
Early Treg proliferation in dLNs is that of amTregs and is MHC class II dependent. (**A**) We adoptively transferred 1-day 4T1 tumor-bearing Thy1.2 mice with naive $CD44^{lo}$ or $CD44^{hi}$ amTregs purified from unmanipulated Thy1.1 BALB/c mice and CFSE labeled prior to inoculation. CFSE proliferation profiles of naive and amTregs among $CD4^+Foxp3^+Thy1.1^+$ donor cells were evaluated at day 5 after adoptive transfer in dLNs and ndLNs. Each panel is representative of 3 mice. (**B**) Proliferation of Tregs at tumor emergence is dependent on MHC class II signaling. MHC-$II^{\Delta/\Delta}$ or C57BL/6 mice with or without 1 day B16F10 tumor received CFSE-labeled Thy1.1 congenic cells from normal mice. Division profiles of $Thy1.1^+$ donor cells were evaluated by flow cytometry at day 6 in dLNs, ndLNs, or nLNs (n = 3 per group). In **A** and **B**, numbers within histograms denote the percentages of $CFSE^-$ and $CFSE^{int}$ cells, as defined in Figure 1A, and corresponding percentages are also shown graphically. *$P < 0.001$ versus respective control.

(38). The activation of Tregs occurred rapidly and thoroughly, while that of Teffs was absent during the first week and then modest (Supplemental Figure 2).

Tregs outrun Teffs at the time of tumor emergence in mice with doxycycline-inducible expression of polyoma middle T oncogene. We further confirmed our observations in a mouse model of spontaneous tumorigenesis, *TetO-PyMT:IRES:Luc;MMTV-rtTA* (referred to herein as *ToMT:IRES:Luc;MTB*; ref. 39). Expression of the polyoma middle T oncogene in the mammary glands of these mice is doxycycline dependent and can be monitored through the coordinate expression of the reporter gene encoding firefly luciferase. Doxycycline-naive animals do not express the transgenic oncogene and have normal mammary glands. Exposure to dietary doxycycline induced immediate mammary expression of the transgenes — as reflected by the appearance of a bioluminescent signal in bitransgenic mice, but not in control animals — and resulted in development of microscopic tumors at day 7 after induction (Figure 3A). We evaluated activation of Tregs and other T cells in this model by coadministering doxycycline and BrdU. In agreement with our findings in transplantable tumor models, spontaneous tumor emergence significantly increased Treg recruitment and division in dLNs compared with ndLNs at day 7 of doxycycline exposure or with nLNs of mice fed doxycycline, but lacking the transactivator transgene (Figure 3B). Very few simultaneously collected $CD4^+Foxp3^-$ or $CD8^+$ T cells from dLNs displayed BrdU incorporation (Figure 3B), resulting in significant reduction in the percentage of $BrdU^+$ Teffs in dLNs compared with ndLNs. The timing of recruitment and activation of Tregs observed in this model was consistent with immune response to tumor emergence, i.e., the first encounter between tumor cells and the immune system.

The early Treg response in dLNs is that of amTregs and is MHC class II dependent. Emerging tumors thus trigger an extremely rapid Treg response, with kinetics reminiscent of a memory-type immune response. This prompted us to test whether this rapid response is generated by the self-reactive amTreg subset, which we previously described as being $CD44^{hi}$ Tregs in mice at the steady state (33). We independently injected purified $CD44^{lo}$ and $CD44^{hi}$ CFSE-labeled Tregs into 4T1 tumor-bearing mice. These 2 Treg populations were equally suppressive in vitro (Supplemental Figure 3). While few $CD44^{lo}$ Tregs had divided at day 5 after injection in both ndLNs and dLNs, 25% of $CD44^{hi}$ Tregs had undergone more than 6 divisions in ndLNs, and greater than 50% had done so in dLNs (Figure 4A). This illustrates the high turnover of the amTreg subset and indicates that they are indeed the cells involved in the early Treg response to tumor emergence.

To investigate whether the recruitment and/or activation of Tregs was driven specifically by antigen recognition or nonspecifically by one or more tumor factors, we evaluated the recruitment and division of CFSE-stained Tregs injected in MHC class II–deficient (MHC-$II^{\Delta/\Delta}$) tumor-bearing mice (40). In this context, we observed that Treg division was totally abrogated (Figure 4B).

The Treg proliferation in dLNs is antigen driven and self specific. To further investigate the antigen specificity of Treg recruitment and/or activation, we transferred Tregs from *TCR-HA* transgenic mice, in which 15%–30% of $CD4^+$ T cells express the 6.5 TCR that is specific for an epitope of influenza hemagglutinin (HA), into syngeneic mice harboring AB1 tumors that did or did not express HA (Figure 5A). At 3 days after transfer, we observed that these Tregs underwent recruitment, activation, and division only in the dLNs of mice implanted with AB1-HA–expressing tumors. Similar results were obtained using the 4T1-HA tumors (Figure 5A). These results indicate that tumor-induced Treg proliferation is antigen driven.

Since tumor-activated Tregs were recruited from the memory pool (Figure 4A) and their activation was antigen driven (Figure 4B and Figure 5A), it is likely that they are self specific rather than tumor specific. To formally prove this, we used a setting where a tumor self antigen is known, transplanting tumor cells with or without HA expression into *InsHA* transgenic hosts (41), and monitored natural HA-specific T cells in the dLN and in tumor-infiltrating lymphocytes (TILs). For that purpose, we developed an assay to detect T cells harboring the specific TCR that was used to generate the *TCR-HA* transgenic mice. Because this TCR likely represents an immunodominant response to HA in BALB/c mice, it may conceivably exist in their wild-type repertoire. We performed a nested PCR that first amplified the proper Vβ-Jβ combination (Vβ8.2-Jβ2.1) and then amplified the specific rearrangement by using a specific primer overlapping the CDR3 junction. We validated this technique by successfully detecting positive signal in the purified Tregs of the pancreatic LNs of untransplanted *InsHA* mice (Figure 5B). Interestingly, in this setting, the signal is 10 times higher in $CD44^{hi}$ memory than in $CD44^{lo}$ quiescent Tregs. Almost no signal was detected in the $CD4^+CD25^-$ cells of the pancreatic LNs or in the Tregs of peripheral LNs. These results also demonstrate that the $CD44^{hi}$ Treg compartment contained self-specific T cells.

We next analyzed the presence of these HA-specific cells in the dLNs and TILs of tumor-bearing mice. At day 5 after transplantation, HA-specific TCR rearrangement was enriched in purified Tregs infiltrating the dLNs and the tumor mass of mice transplanted with HA-expressing tumors compared with animals transplanted with HA-negative tumors or untransplanted controls (Figure 5C). Collectively, these experiments demonstrate that recruitment and activation of Tregs in dLNs was driven by tumor self antigens.

Timely elimination of dividing T cells by antimitotic drugs can result in tumor regression. If the outcome of the battle between Tregs and Teffs appears dictated by their activation kinetics; then (a) ablation of dividing Tregs or (b) presence of amTeffs early at tumor implantation should shift the balance toward more efficient Teff immune responses. We tested this hypothesis by measuring tumor volumes in animals depleted of highly proliferating lymphocytes using hydroxyurea (HU), an antimitotic drug with rapid plasma clearance (Figure 6 and ref. 42). A 3-day HU treatment of tumor-free mice resulted in elimination of 30%–50% of $CD44^{hi}$ Tregs and Teffs, subsets that contain the dividing memory T cells (33, 43), within 5–6 days (Figure 6A). HU had no direct effect on 4T1 tumor growth, as demonstrated in immunodefi-

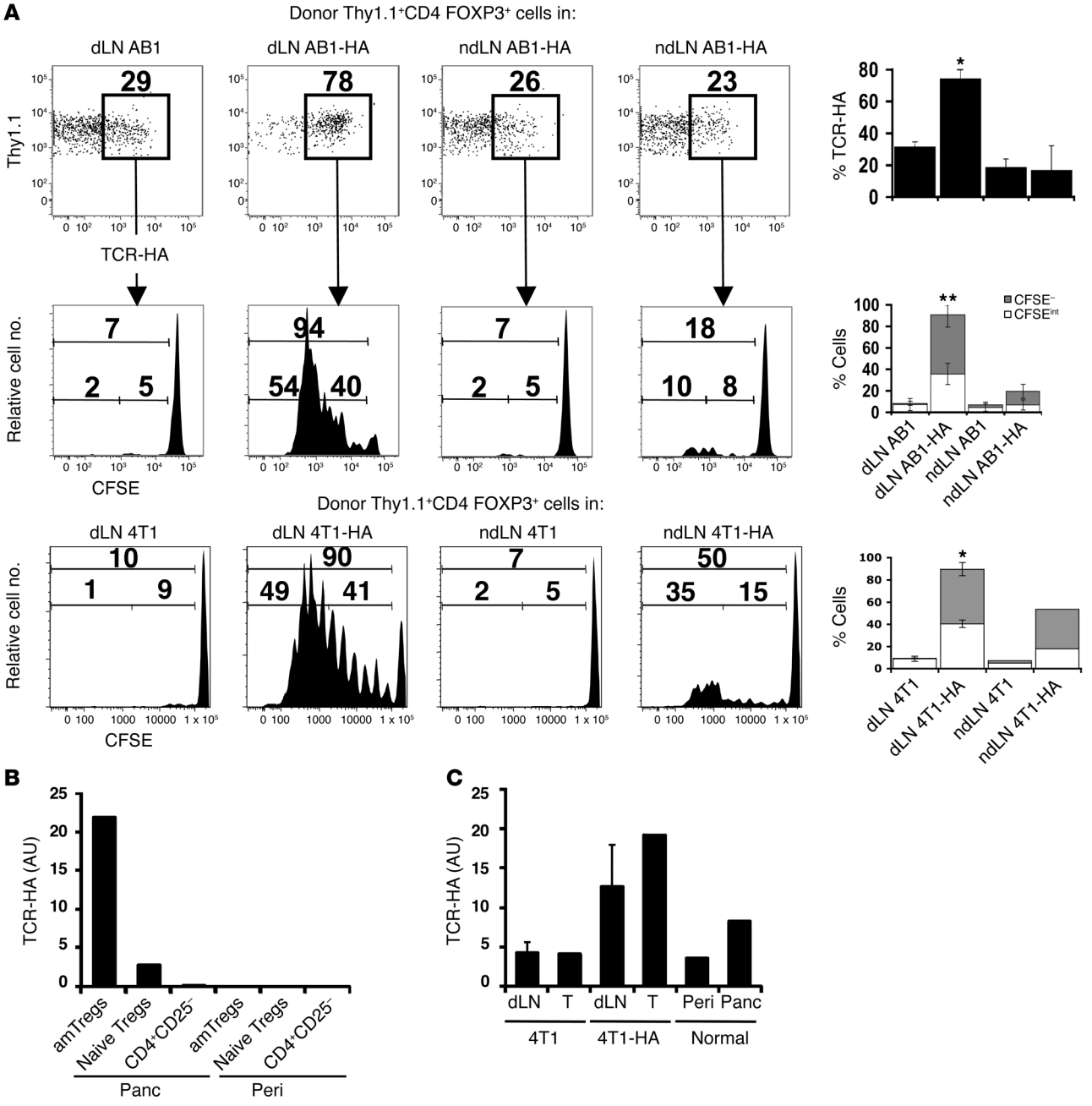

Figure 5

Early accumulation of proliferating Tregs in dLNs is antigen driven and self-antigen specific. (**A**) We adoptively transferred 1-day AB1/AB1-HA or 4T1/4T1-HA tumor-bearing Thy1.2 mice with CFSE-labeled cells from *TCR-HA* Thy1.1 mice. The presence of HA-specific TCR-HA$^+$ cells among CD4$^+$Foxp3$^+$Thy1.1$^+$ Tregs was evaluated at day 3 after adoptive transfer in dLNs and ndLNs, and CFSE profiles were also determined in the 6.5$^+$ subpopulations. Numbers in boxed regions denote 6.5$^+$ cells, and corresponding percentages are also shown graphically. Numbers within histograms denote percent CFSE$^-$ and CFSE^{int} cells, as defined in Figure 1A. Each panel is representative of 3 mice. *$P < 0.01$, **$P < 0.001$ versus respective control. (**B**) CD4$^+$CD25$^-$ T cells, naive CD4$^+$CD25^{hi}CD62L^{hi}CD44^{lo} Tregs, and CD4$^+$CD25^{hi}CD62L^{lo}CD44^{hi} amTregs were sorted from the pancreatic (Panc) or peripheral (Peri) pooled LNs of *InsHA* mice by flow cytometry. cDNAs were used in a Vβ8.2-Jβ2.1 first PCR; products were then amplified by QPCR using TCR-HA clonotype primers. Results are shown relative to wild type. (**C**) Tumor dLNs ($n = 3$) and TILs (pooled) from 5-day 4T1-HA or 4T1 tumor-bearing *InsHA* mice and peripheral or pancreatic LNs ($n = 3$) from normal tumor-free *InsHA* mice were harvested. cDNAs were directly amplified by QPCR using TCR-HA clonotype primers. Results (mean ± SEM) are shown relative to LNs from *TCR-HA* mice, used as a positive control.

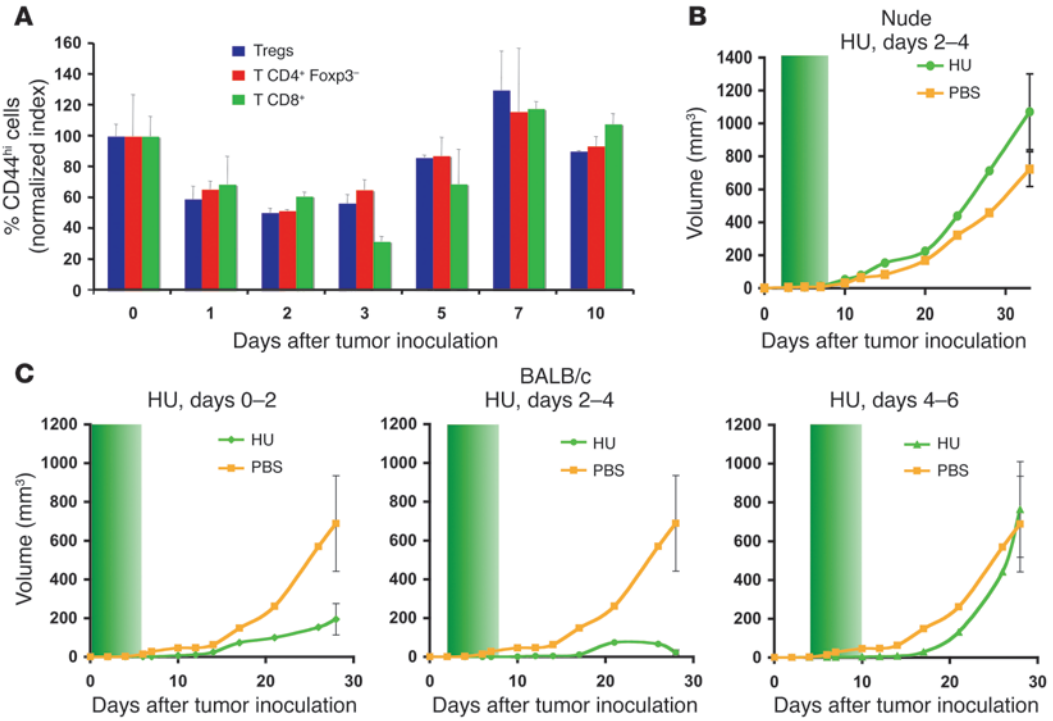

Figure 6

Elimination of proliferating T cells soon after tumor challenge dramatically affects tumor growth. (**A**) Effect of 3 days of HU treatment on the proportion of CD44^{hi} cells in each indicated populations of BALB/c mice, as determined by flow cytometry. Observed percentages were normalized to the untreated control (assigned as 100%) and are shown as mean proportion index ± SEM. (**B** and **C**) HU was administered for 3 consecutive days, leading to depletion of dividing Tregs for a period of 5–6 days (green shading). Volume of 4T1 tumors is shown (n = 6–10 mice per group). (**B**) Treatment by HU did not affect 4T1 tumor growth in nude mice. (**C**) Effect of treatments by HU at days 0–2, 2–4, and 4–6 relative to tumor inoculation in BALB/c mice ($P < 0.0002$, HU versus PBS, for all comparisons).

cient mice (Figure 6B). In contrast, HU given during the first days after tumor implantation into the normal mice markedly reduced tumor growth, in agreement with Treg activation kinetics (Figure 6C). HU given on days 2–4 had the greatest effect. HU given later on had little effect, possibly by affecting both Tregs and Teffs. Similar effects were also observed in the B16F10 tumor model and with other antimitotic drugs such as cyclophosphamide or vinblastine (data not shown). Though correlative, these results suggest that cycling amTregs could be responsible for the inhibition of the antitumor response.

Presence of tumor-specific memory Teffs at the time of tumor emergence shifts the Treg/Teff balance toward efficient antitumor immune responses. To address the effect of preexisting amTeffs on tumor outcome, we used mice that had eradicated a primary tumor after initial depletion of Tregs. These cured mice were able to reject a secondary challenge despite the presence of normal numbers of Tregs (Figure 7A). We tested kinetics of Treg and CD4$^+$Foxp3$^-$ T cell activation and/or proliferation by measuring BrdU incorporation in naive and memory settings. In contrast to our observations in mice challenged with tumor graft for the first time (Figure 2), CD4$^+$Foxp3$^-$ T cells from cured mice were activated with the same kinetics as Tregs (Figure 7B). This led to a considerably lower ratio of BrdU$^+$ Tregs to BrdU$^+$ Teffs in dLNs (Figure 7C), correlated with tumor rejection. However, we did not observe increased expansion of CD8$^+$ T cells in the memory setting at the time of the experiment (day 2 after tumor rechallenge). We made similar observations using the AB1 tumor model (data not shown). These results demonstrate that amTeffs can be activated and multiplied despite Treg engagement, leading to tumor eradication.

Tumor outcome is determined by memory status rather than prevalence of Teffs and Tregs at tumor emergence. To investigate whether tumor growth outcome is determined by the respective number or memory status of Tregs and Teffs, we measured tumor growth upon adoptive transfer of additional Teffs and Tregs. When naive CD25$^-$ T cells from *TCR-HA* transgenic mice were transferred to BALB/c mice 1 day before AB1-HA tumor cell implantation, we observed a delay in tumor growth, correlated with the number of HA-specific transferred T cells, but not tumor rejection, even after transfer of up to 9×10^6 naive HA-specific Teffs (Figure 8A and data not shown). Thus the sole injection of high numbers of naive HA-specific Teffs was not sufficient to reject a tumor. This is in marked contrast with the observation that Treg depletion at tumor inoculation, without transfer of HA-specific Teffs, prevented tumor growth in more than 90% of the treated mice in this tumor model (Figure 8B). However, if the transferred HA-specific Teffs were amTeffs obtained either from mice preimmunized with HA-specific peptide in incomplete Freund adjuvant (IFA), or from mice that had already rejected a primary tumor in the context of Treg depletion (data not shown), the AB1-HA tumors were readily rejected (Figure 8A). Thus, the capacity of Tregs to control Teffs is not a quantitative issue, but rather driven by the memory status of the Teffs.

To test whether resistance of amTeffs to suppression was quantitative or qualitative, we analyzed whether the addition of specific Tregs could overcome the efficient effector responses of amTeffs.

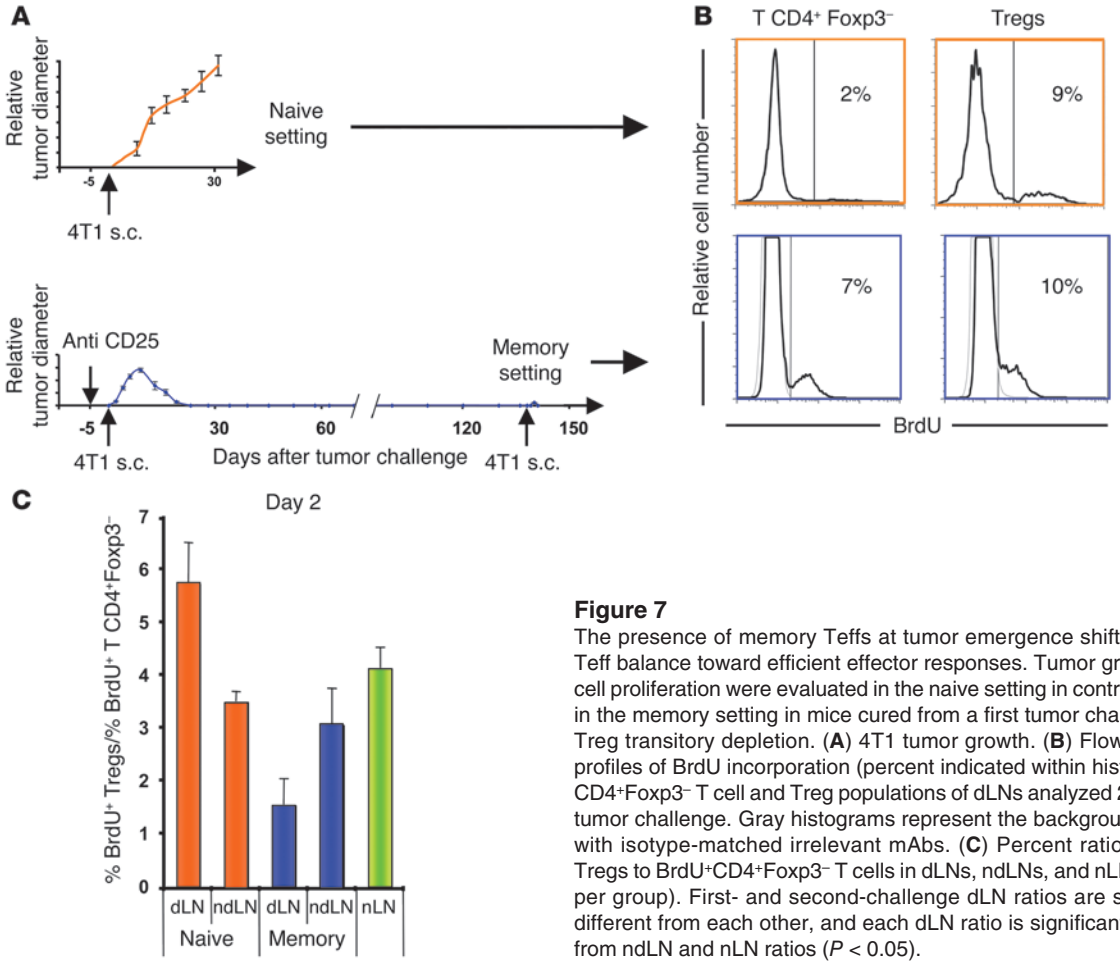

Figure 7
The presence of memory Teffs at tumor emergence shifts the Treg/Teff balance toward efficient effector responses. Tumor growth and T cell proliferation were evaluated in the naive setting in control mice and in the memory setting in mice cured from a first tumor challenge after Treg transitory depletion. (**A**) 4T1 tumor growth. (**B**) Flow cytometry profiles of BrdU incorporation (percent indicated within histograms) in $CD4^+Foxp3^-$ T cell and Treg populations of dLNs analyzed 2 days after tumor challenge. Gray histograms represent the background staining with isotype-matched irrelevant mAbs. (**C**) Percent ratios of $BrdU^+$ Tregs to $BrdU^+CD4^+Foxp3^-$ T cells in dLNs, ndLNs, and nLNs ($n = 3–5$ per group). First- and second-challenge dLN ratios are significantly different from each other, and each dLN ratio is significantly different from ndLN and nLN ratios ($P < 0.05$).

We generated large numbers of cultured HA-specific Tregs obtained from *TCR-HA* transgenic mice, as previously described (44, 45). This culture generated highly enriched 6.5^+ $Foxp3^+$ cells that had extremely potent in vitro (Supplemental Figure 4) and in vivo (44) suppressive activity. Nevertheless, adoptive transfer of high numbers of these cells in mice that had eradicated primary tumor challenge with a HA-expressing tumor (Figure 8B) was insufficient to suppress the secondary response of amTeffs, which did prevent growth of the secondary tumor. We also confirmed in vitro that the amTeffs from cured mice were less sensitive to suppression (Supplemental Figure 5). To confirm the resistance of antitumor amTeffs to Treg suppression, we also analyzed the functionality of Teffs and Tregs sorted based on their expression level of CD44 and CD45RB. We observed that $CD44^{hi}CD45RB^{lo}$ amTeffs from cured mice, but not $CD44^{int}CD45RB^{hi}$ Teffs from naive mice, were indeed quite resistant to Treg suppression both in proliferation and IL-2 secretion (Supplemental Figure 5). Thus, these findings suggest that memory Teffs are intrinsically more resistant to Treg suppression.

Tregs may imprint dominant tolerance at the tumor site. We then investigated whether memory Teffs that can resist amTregs at AB1-HA tumor emergence could efficiently eradicate established tumors at later time points. We first injected anti-HA amTeffs at day 0, 7, 14, and 21 after tumor implantation; except when injected at day 0, these Teffs had no effect on tumor growth, which was only slightly delayed (data not shown). We repeated the experiments injecting cells at days 0, 2, 4 and 6 after tumor implantation and found that amTeffs injected at day 0 or day 2 after tumor implantation efficiently rejected the tumor challenge, while they were inefficient when injected at day 4 or day 6 (Figure 8C).

Discussion

Very little is known about response triggered immediately at the first encounter between immune system and tumor cells. This is surprising, since the orientation of the immune response toward tolerance, Th1 or Th2 response, or allergy is largely influenced by the context encountered when the antigen is first seen (46). We reasoned that the first encounter between tumor cells and the immune system could be the very time when the orientation of the antitumor immune response would be imprinted. We thus focused our study on T cell responses during the first days after tumor emergence. Our results revealed that at this time point, an important battle between Tregs and Teffs takes place that profoundly affects tumor fate. The outcome of the battle appears to depend more on the memory status of the opponents than on their number.

The brisk recruitment of Tregs truly reflects the natural setting of the first encounter between tumor cells and the immune system. We observed brisk recruitment and division of Tregs in the dLN within the first few days of tumor cell implantation in several autologous transplanted mouse tumor models on different genetic backgrounds, validating this observation for the setting of transplanted tumors.

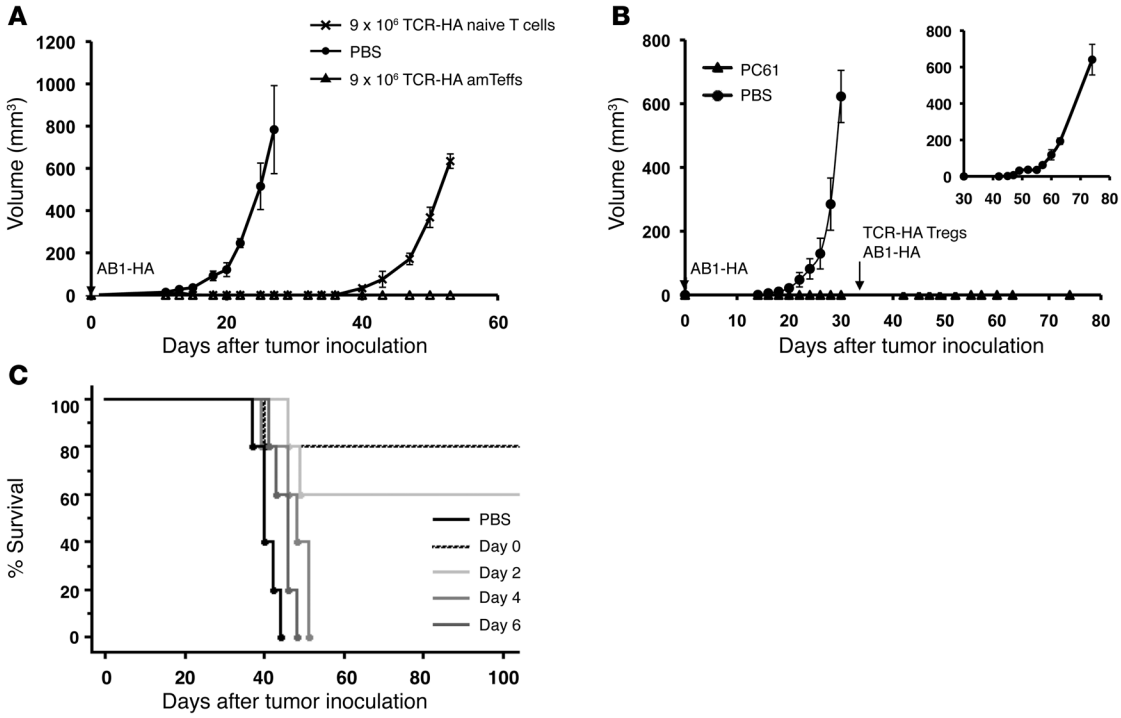

Figure 8

Memory status, rather than number, of antitumor Teffs and Tregs dictates tumor outcome in vivo. (**A**) Mice were challenged with AB1-HA tumor cells and were injected with PBS, with 9 × 10^6 HA-specific CD25$^-$ T cells from unmanipulated *TCR-HA* transgenic mice, or with 9 × 10^6 HA-specific T cells from *TCR-HA* mice immunized with HA in IFA 2 months earlier. Mean tumor volumes ± SEM are shown (n = 5 mice per group). (**B**) Mice were Treg depleted by anti-CD25 Ab treatment and challenged with AB1-HA tumor cells at day 0. Untreated mice developed tumors, whereas treated mice did not. After 30 days, treated cured mice were rechallenged with AB1-HA tumor cells and injected with 5 × 10^6 in vitro–cultured *TCR-HA* Tregs. A new group of age-matched mice was also injected with AB1-HA cells as a control (inset). Previously treated mice did not develop tumors, despite the injection of large numbers of specific Tregs. Mean tumor volumes ± SEM are shown (n = 5 mice per group; 3 experiments). (**C**) Addition of *TCR-HA*–activated amTeffs was sufficient to reject AB1-HA tumor only when injected between day 0 and day 4. BALB/c mice were injected s.c. with 5 × 10^5 AB1-HA or AB1 at day 0 and i.v. with PBS, or with 5 × 10^6 *TCR-HA* T cells from immunized *TCR-HA* mice at day 0, 2, 4, or 6 (n = 5 per group).

Although transplantable tumors have long been integral to tumor immunology research, they have several characteristics that limit their applicability to human disease, in particular because injection of tumor cells, even in low numbers, does not fully mimic spontaneous emergence of tumors. However, long latencies and absence of reliable early detection protocols for tumors in traditional mouse models of spontaneous chemically induced tumorigenesis makes them poorly suited for studies of nascent tumor immunity. Some indication that the preeminence of Treg activation is not a result of tumor cell injection or an artifact induced by in vitro culture conditions comes from the lack of detectable Treg response to allogeneic tumors grafted using the identical injection procedure (data not shown).

We were able to further address these problems using a doxycycline-inducible model of mammary tumorigenesis. In our model, expression of a potent oncogene, polyoma middle T, is absolutely dependent on the presence of a product of another transgene, *MMTV-rtTA*, and the small molecule doxycycline, in whose absence mammary tissue of bitransgenic mice remains phenotypically and functionally normal (39). Yet the expression of the polyoma middle T oncogene localized in mammary epithelium of adult bitransgenic mice induces rapid malignant transformation and emergence of numerous microscopic tumors in all 10 mammary glands within days of exposure to dietary doxycycline. The experimental control over the exact timing of tumorigenesis afforded by this model allowed us to study early tumor immunity in surgically unmanipulated, transplant-free mice and to confirm preferential activation of Treg responses in the LNs draining tumor-bearing mammary glands.

Early recruitment and expansion of Tregs in the dLNs of bitransgenic tumor-bearing mice at day 7 after oncogene induction was comparable to that observed in our transplantable models at day 3 after tumor cell injection. Similarly, early Treg activation in the inducible model occurred in the virtual absence of detectable Teff responses. Evidence for early Treg activation in the inducible tumor model strengthens our observations made with the transplanted tumors and underscores their relevance to understanding the first encounter between the immune system and cancer cells.

In various experiments we have observed that the adoptive transfer of Tregs, whether naive or amTregs, and even in vast quantities, at best modestly enhance tumor growth (data not shown); this indicates that there are already enough Tregs in the natural setting to block the effector responses that could impede tumor growth.

The subset of self-reactive CD44^{hi} amTregs is responsible for early induction of tumor immunity. Multiple lines of evidence point to the existence of a population of self-reactive Tregs that have an acti-

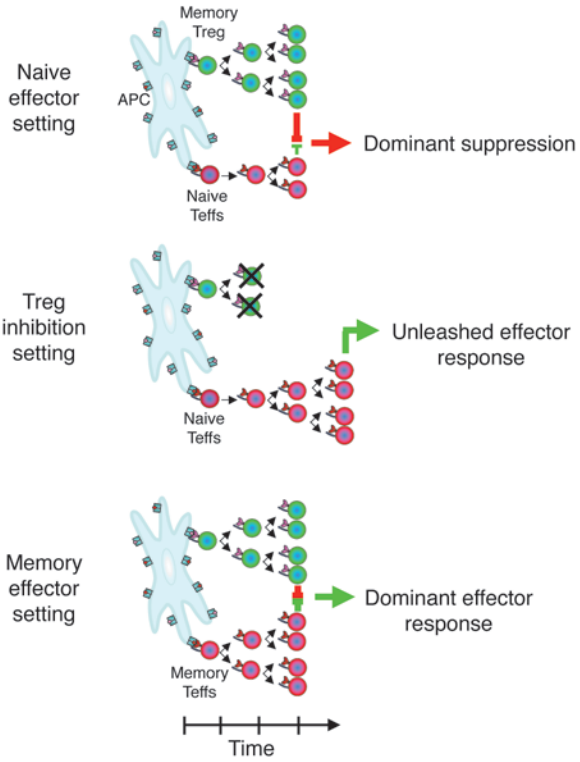

Figure 9
Simplified model of the immune tolerance versus immune rejection decision process based on activation kinetics and memory status.

vated/memory phenotype (47, 48). We initially reported that in the steady state, these amTregs have a very rapid turnover and are $CD44^{hi}$ (33). In the present work, we extend these observations and show that the $CD4^+CD25^{hi}CD62L^{lo}CD44^{hi}$ T cells were Foxp3-expressing bona fide Tregs (Supplemental Figure 3) and that when purified populations of $CD44^{hi}$ or $CD44^{lo}$ Tregs were separately injected in normal mice, only the $CD44^{hi}$ subset divided intensely in LNs. We show that these amTregs — although not the $CD44^{lo}$ ones — were those actively dividing in the dLN. This raises the question of the specificity of amTreg activation in this setting.

We previously reported that when Tregs from *TCR-HA* mice, carrying a transgenic TCR specific for HA, were transferred to *InsHA* mice that express HA in the pancreatic islet, the migration and subsequent cycling of Tregs was preferentially detected in the pancreatic LNs (33). Similarly, when Tregs from *TCR-HA* mice were injected in mice bearing tumors with or without HA, we found preferential recruitment and division of Tregs in the HA-expressing dLNs. Thus, we conclude that the early Treg recruitment and division in dLNs is antigen mediated, rather than the result of release of nonspecific factors and/or cytokines by the tumor. However, cytokines like TGF-β or IL-10 could play an important role in the subsequent vigorous and continuous proliferation and migration of Tregs to the tumor site after their initial reactivation (8, 49). Incidentally, although in vitro Treg proliferation is strictly IL-2 dependent, the role of IL-2 for amTreg proliferation in vivo remains to be deciphered; basal levels of IL-2 secretion could be provided by the $CD4^+CD25^{lo}$ conventional T cells (50) or by DCs that migrate from the tumor site to present antigens (51).

Nature of the antigens recognized by amTregs that suppress the antitumor effector responses. Accumulation of mutations alters cancer cell proteome (52) and can result in changes in antigen processing and presentation of self antigens usually ignored by the immune system (53) as well as expression of new antigens or reexpression of embryonic antigens, which can be considered as non-self by the immune system. However, cancer cells continue to express self-antigens known to the immune system and therefore can also be targeted by Tregs, which express a broadly polyclonal (21, 54) but self-specific repertoire (55). In addition, it has recently been shown that physiologic self antigens rapidly capacitate self-specific polyclonal Tregs for control of organ-specific autoimmune diseases and that Tregs that have already encountered their cognate Ag have improved functional capacities compared with naive Tregs (34, 56). It has also been shown that Tregs responding to serologically defined autoantigens suppress antitumor immune responses and accelerate tumor development (25, 28). Thus, given that Tregs involved in the antitumor response appear to be amTregs generated in animals that have not seen the tumor, and thus have not previously encountered the potential tumor-specific antigens, and that the kinetics of the Treg response is that of a memory response, the tumor-driven early Treg response must be triggered by antigens shared by the tumors and normal cells, i.e., normal self antigens.

Moreover, we formally proved that self-specific Tregs were recruited to the tumor. By using quantitative PCR (QPCR) detecting the T cells expressing a HA-specific TCR, we detected HA-specific Tregs but no conventional helper T cells among the TILs of HA tumor–bearing *InsHA* mice. Since HA is an autoantigen for *InsHA* mice, this proves that the self-specific amTregs are recruited during the antitumor immune response.

It is noteworthy that the detection of specific T cells by QPCR should be valuable for monitoring various types of T cell–mediated immune responses. This could be of special relevance for the study of CD4 responses, since class II tetramers are not yet widely available. This technique may also prove to be more sensitive than tetramer analyses and could also be adapted to detect specific TCRs at the single-cell level (22).

In a natural setting, self antigens recognized by the tumor-recruited self-specific Tregs are largely unknown. It is thus difficult to determine if tumor-induced amTreg activation is mediated by a restricted or rather an extensive set of self antigens. However, it was reported that Tregs from human dLNs display a polyclonal TCR Vβ-chain repertoire (21), and our preliminary studies indicate that $CD44^{hi}$ Treg repertoire is quite diverse and does not undergo much clonal expansion in the dLNs (our unpublished observations). Because of this, and of the magnitude of the Treg response, we favor the hypothesis that the tumor-driven early Treg response is a polyclonal response triggered by a large set of self antigens. For example, in the model of recruitment of HA-specific Tregs to dLNs of HA-tumor bearing *InsHA* transgenic mice, the HA transgene represents one of many endogenous self antigens expressed in the developing thymus of transgenic animals by an AIRE-dependent mechanism (57) and poised to induce positive selection of Tregs (58). Hence the recruitment of HA-specific Tregs in the dLN and their presence among HA-tumor TILs strongly suggests that the repertoire of tumor-recruited Tregs is vast.

The respective memory status and activation kinetics of Tregs and Teffs determine tumor outcome. The effector response to tumor cells is mediated by naive T cells. Indeed, significant activation and division of $CD4^+Foxp3^-$ or $CD8^+$ T cells in dLNs was

not observed sooner than 9–12 days after tumor implantation, regardless of whether Tregs had been depleted (Figure 1 and data not shown). Because naive Teffs have a lower global reactivity to antigens than amTeffs (59, 60) and amTregs have enhanced suppressive activity compared with naive Tregs (61, 62), it is not surprising that memory-type Treg responses dominated primary-type Teff responses. These observations suggest that in a setting where there would be some memory Teffs, the outcome of the Teff/Treg battle could be different. Response to a secondary tumor challenge in mice that had survived a primary tumor rejection after Treg depletion offered a perfect setting to study this hypothesis. Indeed, the initial tumor rejection we observed is likely to have generated and expanded memory Teffs, as supported by the observation that these mice spontaneously rejected secondary tumor challenge and that their T cells responded better than naive T cells to stimulation with tumor lysate–sensitized DCs. As predicted, we observed equally rapid and efficient Teff and Treg activation upon secondary tumor challenge as well as stronger resistance to Treg suppression that led to tumor eradication by the activated Teffs. These results further underscore potential efficiency of properly activated and expanded antitumor Teffs; they are in line with the observations that immunization against a tumor-specific antigen led to induction of amTeffs, at levels sufficient to protect mice from primary tumor challenge despite the presence of Tregs. These results thus suggest that a modification of the balance between Tregs and Teffs can change tumor outcome.

The net result of Treg and Teff activation in response to cancer seems to be driven by qualitative more than quantitative aspects of the T cell subsets. Indeed, injection of large numbers of tumor antigen–specific naive Teffs before tumor implantation did not overcome the Treg barrier; thus, amTregs dominated naive Teffs, irrespective of their numbers. On the contrary, once amTeffs were present, injection of large numbers of tumor antigen–specific activated Tregs failed to overcome Teff response; thus, amTeffs could not be controlled by amTregs, irrespective of their numbers. Hence, the quality of global antitumor response mostly depends on the immunological memory status of Teffs and Tregs. Indeed, we showed that antitumor amTeffs appeared to be less sensitive to Treg suppression of proliferation and of IL-2 production in vitro than did naive Teffs (Supplemental Figure 5). We also observed the appearance of a marked population of helper $CD4^+$ T cells producing both IL-2 and IFN-γ (data not shown), such IFN-γ–producing $CD4^+$ T cells being of prime importance in efficient antitumor immunity (63, 64).

These results are in line with those of Yang et al., who reported that allograft rejection mediated by memory T cells is resistant to regulation by Tregs (65). Nishikawa and colleagues also observed that $CD45RO^+$ tumor-specific $CD4^+$ T cells are more resistant to Tregs than are $CD45RA^+$ tumor-specific $CD4^+$ T cells in cancer patients (66). This resistance could be in part due to the fact that activated Tregs can downregulate expression of costimulation molecules by DC (67), and amTeffs are much less dependent on costimulation than naive T cells (68). They also can be viewed as a mirror image of the findings of Korn and colleagues in the autoimmune model of EAE (69): both Tregs and Teffs expanded in the peripheral lymphoid compartment and readily accumulated in the CNS, but Tregs did not prevent the onset of disease. Tregs isolated from the CNS were effective in suppressing naive myelin oligodendrocyte glycoprotein–specific T cells, but failed to control CNS-derived encephalitogenic amTeffs (69). Together, these observations suggest that amTeffs could be inherently more resistant to Tregs.

Thus, the outcome of the immune response developed against tumor cells is all about déjà vu. This explains an old paradigm of cancer immunology — that preventive immunization is more effective than therapeutic immunization — and suggests that preventive vaccination against cancer should be reconsidered. Preventive vaccination with tumor-specific antigen presented in a context that would not stimulate amTregs should allow for the development of efficient memory Teffs, which are able to mount efficient effector responses when a tumor emerges. Also noteworthy is the previous finding that detection of memory Teffs correlated with good prognosis in cancer patients (70, 71). However, in the therapeutic setting, the battle and race between Tregs might not turn easily to the advantage of Teffs, even if they are activated/memory cells. Indeed, although amTeffs cannot be controlled by Tregs, if they are injected at the time of tumor implantation, they lose this ability when injected just a few days later. This suggests that the early rapid recruitment of Tregs could imprint a dominant tolerant environment, either in the dLN or at the tumor site (22). Our preliminary results indicate that appearance of this dominant tolerance coincides with upregulated expression of indoleamine 2,3-dioxygenase (IDO), a molecule that has clearly been associated with tumor resistance to effector immune responses (72), in the tumor microenvironment (our unpublished observations). Alternatively, it is possible that, while Treg resistant, the am Teffs could only function prophylactically when tumor is small enough to be attacked efficiently. This would pose major problems for the development of efficient immunotherapy of cancer.

Revision of the immunosurveillance concept. We show here that relative activation speed of self-specific memory Tregs versus that of tumor-specific naive Teffs at the time of tumor emergence dictates tumor outcome. At this stage, the aberrant-self nature of tumor cells is less important to the immune system than their normal-self nature, which in fact triggers remarkably strong regulatory immune response. There is clearly no immune ignorance of tumors. There is, however, obvious immune surveillance at work: a caveat aimed at tolerance induction. Such immunosurveillance may well find its roots in evolution-driven development of mechanisms to protect cells, such as fetal cells, that are simultaneously normal and abnormal to the immune system. More generally, our results highlight the importance of timing of the Treg and Teff engagement — which depends on their memory status — on the outcome of an immune response. We propose a model in which, besides the role of T cell repertoire selection or danger signals, the fate of the immune responses toward tolerance or rejection is also driven by the respective memory status of the players (Figure 9).

Methods

Transplanted tumor models. Female BALB/c, BALB/c-nude, and C57BL/6 mice (6–8 weeks old) were obtained from Charles River Laboratories. Thy-1.1 BALB/c, Thy-1.1 C57BL/6, and Ly5.1 C57BL/6 congenic mice; *InsHA* mice (41); *TCR-HA*×Thy-1.1 mice (33), derived from TCR-HA mice recognizing I-E–restricted HA epitope 110–120 (SFERFEIFPKE; provided by H. von Boehmer, Dana-Farber Cancer Institute, Harvard Medical School, Boston, Massachusetts, USA); and MHC-$II^{\Delta/\Delta}$ mice (provided by M. Nussenzweig, Rockefeller University, New York, New York, USA) were maintained in our animal facility. Mice were housed in filter-topped cages under specific pathogen–free conditions. All mice were treated in accordance with the

European Union guidelines for animal experimentation, and the present studies were reviewed and approved by the Charles Darwin institutional review board of the CNRS. Survival was determined by the time at which mice required euthanasia, when tumor diameter reached 15–20 mm.

The 4T1 tumor cell line (provided by S. Ostrand-Rosenberg, University of Maryland Baltimore County, Baltimore, Maryland, USA), derived from a BALB/c spontaneous mammary carcinoma, and its 4T1-HA derivative that express the murine influenza HA were cultured in Iscove modified Dulbecco medium (Gibco; Invitrogen) supplemented with 10% FCS (PAA Laboratories) and 1% gentamicin (Gibco; Invitrogen). The B16F10 tumor cell line, derived from a C57BL/6 melanoma, was obtained from the ATCC (catalog no. CRL-6475) and cultured in DMEM (Gibco; Invitrogen) complemented with 10% FCS, 2 mM L-glutamine (Gibco; Invitrogen), and 100 U/ml penicillin-streptomycin (Gibco; Invitrogen). The AB1 tumor cell line, derived from a BALB/c malignant mesothelioma (73), and its AB1-HA derivative (74) were supplied by B. Scott (Centre for Functional Genomics and Human Disease, Monash Institute of Medical Research, Clayton, Victoria, Australia). All cell lines were mycoplasma free.

For in vivo experiments, 1×10^5 (4T1, 4T1-HA, B16F10) or 5×10^5 (AB1, AB1-HA) tumor cells were injected s.c. in the left flank of a mouse. Tumor volume was determined by measuring perpendicular tumor diameters L and l using vernier calipers, calculated as $(L \times l^2)/2$, and expressed as mm^3. The left inguinal LN was used as the dLN. The right inguinal and/or bilateral axillary LNs were used as ndLNs.

Doxycycline-inducible tumor model. Mice bearing the *MMTV-rtTA and TetO-PyMT:IRES:Luc* transgenes and their genotyping protocols have been previously described (39, 75). Doxycycline was administered by feeding mice with doxycycline-impregnated food pellets (625 ppm; Harlan-Teklad). Mice were placed on doxycycline as indicated for particular experiments. Inguinal, axillary, and brachial LNs were used as dLNs, and pancreatic, sacroiliac, and lumbar LNs were used as ndLNs.

In vivo bioluminescent imaging. Mice were anesthetized with 3% isoflurane and injected retro-orbitally with 50 μl of 30 mg/ml D-luciferin (catalog no. XR-1001; Caliper Life Sciences) in sterile water. Bioluminescence images were acquired with the IVIS Imaging System (Xenogen) 2–5 minutes after injection. Acquisition time was set to 1 second. Analysis was performed using LivingImage software (version 3.0; Xenogen) by measurement of photon flux (measured in photons/s/cm^2/steradian).

HA immunization. *TCR-HA* transgenic mice were immunized s.c. on the right (50 μg) and left (50 μg) flanks and at the base of the tail (100 μg) with the I-E–restricted HA epitope 110–120 in IFA. After 2 months, mice were sacrificed, and the spleens and inguinal/popliteal LNs were harvested.

In vivo depletion of $CD4^+CD25^+$ T cells and cycling cells. Treg ablation was performed by i.p. injection of 125 μg of the anti-CD25 mAb PC61 2 or 5 days before tumor challenge in the 4T1 and B16F10 models and at the time of tumor challenge in the AB1 model. This induces a greater than 80% transient depletion of LN $CD25^{hi}$ cells for approximately 4 weeks in normal mice (76). In the experiments shown in Figure 1, however, C57BL/6 mice twice received 1 mg PC61 Ab at day –4 and day –2, as described previously (5). HU (Hydrea; Bristol-Myers Squibb) was administered at the dose of 1 g/kg/d, as a cycle of 2 i.p. injections given 7 hours apart.

Abs and flow cytometry analyses. Cells from peripheral LNs obtained after a mechanical dissociation were processed as described previously (33) and then stained with saturating amounts of combinations of the following mAbs (all from BD Biosciences): peridinin-chlorophyll-protein– (PerCP-), allophycocyanin- (APC-), or APC–cyanin 7–labeled (APC-Cy7–labeled) anti-CD4; PerCP- or CyChrome-labeled anti-CD8; PE- or APC-labeled antiCD25; PE-labeled anti-Ly5.1/CD45.1; PerCP-labeled anti–Thy-1.1/CD90.1; and PE-Cy7–labeled CD44. We also used the following biotinylated Abs (all from BD Biosciences): anti-CD25, anti-CD69, and anti–Thy-1.1/CD90.1. Labeling with the anticlonotypic mAb (clone 6.5) specific to TCR-HA was revealed by a biotin anti-rat IgG2b mAb and streptavidin-CyChrome (BD Biosciences — Pharmingen). The biotinylated mAbs were detected by Pe-Cy7, PerCP-streptavidin, or APC-streptavidin (BD Biosciences). BrdU labeling was performed as described previously (33). Intracellular labeling of transcription factor Foxp3 by anti-Foxp3 conjugated to PE or Pacific Blue (FJK-16s; eBioscience) was performed according to the manufacturer's recommendations. Isotype-irrelevant mAbs were used as controls. For FoxP3 and BrdU costaining experiments, samples were incubated for 30 minutes at room temperature with 1 mg/ml DNase1 before intracytoplasmic labeling.

Lymphocytes were analyzed with FACSCalibur or LSR-II (BD Biosciences). Further analyses were performed with FlowJo software (version 8.3.3; Tree Star). After adoptive transfer in wild-type hosts under our experimental conditions, donor Tregs represented 0.1% of splenocytes or LN cells (33). Therefore, $1–3 \times 10^6$ events were acquired for each analysis.

BrdU labeling. Mice were injected i.p. twice a day with 1 mg of the nucleoside analog BrdU (Sigma-Aldrich) for 1–5 days. Detection of BrdU incorporation in DNA of cycling cells was performed by flow cytometry as described previously (33). For long-term labeling in the inducible tumor model, mice continuously received BrdU at 40 mg/ml in drinking water.

CFSE staining and adoptive transfer of cells. Cells were labeled with CFSE (Sigma-Aldrich) as described previously (33) and transferred i.v. to mice. Adoptive transfer was performed with either (a) unpurified cells from Thy1.1 congenic mice that were further analyzed after transfer in Thy1.2 mice based on Foxp3 and Thy1.1 expression to identify donor Tregs, or (b) $CD4^+CD25^+$ and $CD25^-$ cells from LNs and spleens of Thy1.1 congenic C57BL/6, BALB/c, or *TCR-HA* mice or from Ly5.1 congenic C57BL/6 mice, which were purified by MACS using a $CD4^+CD25^+$ T cell isolation kit (Miltenyi Biotec) and eventually by sorting using a FACSAria flow cytometer (BD Biosciences) as previously described (33). Because approximately 90% of $CD4^+CD25^+$ T cells were $Foxp3^+$ and less than 1% of $CD4^+CD25^-$ T cells were $Foxp3^+$ in normal untreated mice (data not shown), $CD25^+$ and $CD25^-$ $CD4^+$ T cells fractions were considered to be Tregs and $CD4^+$ Teffs, respectively.

TCR-specific QPCR assays. 4T1-HA or 4T1 tumor cells were injected s.c. in *InsHA* mice at day 0. After 5 days, mice were sacrificed, and pancreatic LNs, peripheral LNs, dLNs, and TILs were harvested. Cells were sorted on a FACSAria cytometer (BD Biosciences) based on the CD4, CD25, CD44, and CD62L markers as $CD4^+CD25^-$ Teffs, $CD4^+CD25^{hi}CD44^{lo}CD62L^{hi}$ naive Tregs, or $CD44^{hi}CD62L^{lo}$ amTregs. We verified than 90% of sorted $CD4^+CD25^{hi}CD44^{hi}CD62L^{lo}$ T cells expressed Foxp3 and were bona fide memory Tregs (Supplemental Figure 3). Total mRNA was prepared from tissues using TRIZOL reagent (Invitrogen) and phenol chloroform extraction. RT-PCR was performed to synthesized cDNA for PCR analysis.

TCR-HA cDNA in each sample was quantified by real-time QPCR (Applied Biosystems). The primers for the TCR-HA gene first amplification were forward primer Vβ8.2, 5′-ACAAGGTGGCAGTAACAGGA-3′, and reverse primer Jβ2.1, 5′-CCTCTAGGACGGTGAGTCGTG-3′. For the nested QPCR, the forward primer Vβ8.2 was 5′-AGTTGGCTACCCCCTCTCAGA-3′, the reverse primer was 5′-GGCCGGGGGAGTTATGC-3′, and the probe labeled with fluorescent reporter was 5′-FAM-ATCAGTGTACTTCTGTGCCAGCGGTGG-TAMRA-3′. As an internal control, endogenous mouse *HPRT* was also amplified: forward, 5′-CACGTGGGCTCCAGCATT-3′; reverse, 5′-TCACCAGTCATTTCTGCCTTT-3′; probe, 5′-FAM-CCAATGGTCGGGCACTGCTCAA-TAMRA-3′. Primers and probes were designed with Primer Express software (version 1.5; Applied Biosystems). Real-time PCR was performed twice using TaqMan Universal PCR master mix (Applied Biosystems) with 200 ng of equivalent mRNA in case of nested QPCR or 600 ng of equivalent mRNA in case of classic direct QPCR. The average Ct of the

triplicates was used to calculate the fold change relati ve to positive control cDNA of cells from *TCR-HA* mice.

In vitro Treg expansion. HA-specific Tregs were obtained by sorting $CD62L^{hi}CD25^{hi}CD4^+$ T cells from *TCR-HA* transgenic mice using a FACSAria cytometer (BD Biosciences). Tregs were then cultured in vitro with murine IL-2 (R&D Systems) and HA-loaded $CD11c^+$ DCs as described previously (44). Tregs were then used in in vitro assays or injected i.v. in mice. Fluorescence-activated cell sorting (FACS) analysis and suppression assay were used to verify the phenotype and the in vitro function of these cells.

Peptide-specific and polyclonal suppression assays. For the polyclonal specific suppression assays, 5×10^4 FACS-sorted $CD4^+CD25^-$ T cells were cocultured with different ratios of $CD4^+CD25^+CD44^{hi}CD62L^{lo}$ amTregs or $CD4^+CD25^+CD44^{lo}CD62L^{hi}$ Tregs from BALB/c mice and anti-CD3/anti-CD28 mAbs in 96-well round-bottomed plates for 2–3 days. For the peptide-specific suppression assay, 4×10^4 or 5×10^4 $CD4^+CD25^-$ T cells sorted by FACS or magnetic-activated cell sorting were cocultured with different ratios of Tregs from BALB/c mice or from culture and $1–2.5 \times 10^4$ HA-loaded magnetically purified $CD11c^+$ DCs in 96-well round-bottomed plates for 2–3 days. In both assays, cells were pulsed for the last 8 hours with ^{3}H-methyl thymidine (2 μCi per well; Amersham), and radioactivity was measured by a Beckman liquid scintillation counter.

Statistics. Statistical analyses of survival curves were performed using the log-rank test. Data comparison of 1 and 2 variables was performed using 1- and 2-way ANOVA, respectively, with Bonferroni adjustment. We evaluated statistical significance with Prism software (version 5.01; GraphPad Software Inc.). Unless otherwise indicated, data are expressed as mean ± SD. A P value less than 0.05 was considered statistically significant.

Acknowledgments

We thank Suzanne Ostrand-Rosenberg for providing the 4T1 tumor cell line, Bernadette Scott for providing the AB1±HA tumor cell line, Harald von Boehmer for providing the *TCR-HA* transgenic mice, and Michel Nussenzweig for providing the MHC-$II^{\Delta/\Delta}$ mice. This work was supported by the Ministère de la Recherche, Université Pierre and Marie Curie (Paris VI), the Association pour la Recherche sur le Cancer (ARC), and the CNRS. We thank Charlotte Dalba for critical reading of the manuscript, Béatrice Clerc and Beatrice Levacher for their contributions to some of the experiments, Bruno Gouritin and Sylvie Grégoire for assistance with flow cytometry sorting, and Brice Chanudet and Pierric Parent for animal care.

Received for publication June 30, 2008, and accepted in revised form May 20, 2009.

Address correspondence to: David Klatzmann, Hôpital Pitié-Salpêtrière, 83 Bd de l'Hôpital, Paris 75651, France. Phone: 33-1-42-17-74-61; Fax: 33-1-42-17-74-62; E-mail: david.klatzmann@upmc.fr.

1. Ochsenbein, A.F., et al. 1999. Immune surveillance against a solid tumor fails because of immunological ignorance. *Proc. Natl. Acad. Sci. U. S. A.* **96**:2233–2238.
2. Burnet, M. 1957. Cancer: a biological approach. III. Viruses associated with neoplastic conditions. IV. Practical applications. *Br. Med. J.* **1**:841–847.
3. Willimsky, G., and Blankenstein, T. 2005. Sporadic immunogenic tumours avoid destruction by inducing T-cell tolerance. *Nature.* **437**:141–146.
4. Yamaguchi, T., and Sakaguchi, S. 2005. Regulatory T cells in immune surveillance and treatment of cancer. *Semin Cancer Biol.* **16**:115–123.
5. Shimizu, J., Yamazaki, S., and Sakaguchi, S. 1999. Induction of tumor immunity by removing CD25+CD4+ T cells: a common basis between tumor immunity and autoimmunity. *J. Immunol.* **163**:5211–5218.
6. Curiel, T.J., et al. 2004. Specific recruitment of regulatory T cells in ovarian carcinoma fosters immune privilege and predicts reduced survival. *Nat. Med.* **10**:942–949.
7. Chen, M.L., et al. 2005. Regulatory T cells suppress tumor-specific CD8 T cell cytotoxicity through TGF-beta signals in vivo. *Proc. Natl. Acad. Sci. U. S. A.* **102**:419–424.
8. Ghiringhelli, F., et al. 2005. Tumor cells convert immature myeloid dendritic cells into TGF-beta-secreting cells inducing CD4+CD25+ regulatory T cell proliferation. *J. Exp. Med.* **202**:919–929.
9. Wolf, D., et al. 2005. The expression of the regulatory T cell-specific forkhead box transcription factor FoxP3 is associated with poor prognosis in ovarian cancer. *Clin. Cancer Res.* **11**:8326–8331.
10. Sato, E., et al. 2005. Intraepithelial CD8+ tumor-infiltrating lymphocytes and a high CD8+/regulatory T cell ratio are associated with favorable prognosis in ovarian cancer. *Proc. Natl. Acad. Sci. U. S. A.* **102**:18538–18543.
11. Fontenot, J.D., Gavin, M.A., and Rudensky, A.Y. 2003. Foxp3 programs the development and function of CD4+CD25+ regulatory T cells. *Nat. Immunol.* **4**:330–336.
12. Hori, S., Nomura, T., and Sakaguchi, S. 2003. Control of regulatory T cell development by the transcription factor Foxp3. *Science.* **299**:1057–1061.
13. von Boehmer, H. 2005. Mechanisms of suppression by suppressor T cells. *Nat. Immunol.* **6**:338–344.
14. Miyara, M., and Sakaguchi, S. 2007. Natural regulatory T cells: mechanisms of suppression. *Trends Mol. Med.* **13**:108–116.
15. Sakaguchi, S. 2005. Naturally arising Foxp3-expressing CD25+CD4+ regulatory T cells in immunological tolerance to self and non-self. *Nat. Immunol.* **6**:345–352.
16. Belkaid, Y., and Rouse, B.T. 2005. Natural regulatory T cells in infectious disease. *Nat. Immunol.* **6**:353–360.
17. Karlsson, M.R., Rugtveit, J., and Brandtzaeg, P. 2004. Allergen-responsive CD4+CD25+ regulatory T cells in children who have outgrown cow's milk allergy. *J. Exp. Med.* **199**:1679–1688.
18. Cohen, J.L., Trenado, A., Vasey, D., Klatzmann, D., and Salomon, B.L. 2002. CD4(+)CD25(+) immunoregulatory T Cells: new therapeutics for graft-versus-host disease. *J. Exp. Med.* **196**:401–406.
19. Berendt, M.J., and North, R.J. 1980. T-cell-mediated suppression of anti-tumor immunity. An explanation for progressive growth of an immunogenic tumor. *J. Exp. Med.* **151**:69–80.
20. Orentas, R.J., Kohler, M.E., and Johnson, B.D. 2006. Suppression of anti-cancer immunity by regulatory T cells: back to the future. *Semin. Cancer Biol.* **16**:137–149.
21. Viguier, M., et al. 2004. Foxp3 expressing CD4+CD25(high) regulatory T cells are overrepresented in human metastatic melanoma lymph nodes and inhibit the function of infiltrating T cells. *J. Immunol.* **173**:1444–1453.
22. Chaput, N., et al. 2007. Regulatory T cells prevent CD8 T cell maturation by inhibiting CD4 Th cells at tumor sites. *J. Immunol.* **179**:4969–4978.
23. Onizuka, S., et al. 1999. Tumor rejection by in vivo administration of anti-CD25 (interleukin-2 receptor alpha) monoclonal antibody. *Cancer Res.* **59**:3128–3133.
24. Golgher, D., Jones, E., Powrie, F., Elliott, T., and Gallimore, A. 2002. Depletion of CD25+ regulatory cells uncovers immune responses to shared murine tumor rejection antigens. *Eur. J. Immunol.* **32**:3267–3275.
25. Nishikawa, H., et al. 2005. Accelerated chemically induced tumor development mediated by CD4+CD25+ regulatory T cells in wild-type hosts. *Proc. Natl. Acad. Sci. U. S. A.* **102**:9253–9257.
26. Dannull, J., et al. 2005. Enhancement of vaccine-mediated antitumor immunity in cancer patients after depletion of regulatory T cells. *J. Clin. Invest.* **115**:3623–3633.
27. Sharma, M.D., et al. 2007. Plasmacytoid dendritic cells from mouse tumor-draining lymph nodes directly activate mature Tregs via indoleamine 2,3-dioxygenase. *J. Clin. Invest.* **117**:2570–2582.
28. Nishikawa, H., et al. 2003. CD4+ CD25+ T cells responding to serologically defined autoantigens suppress antitumor immune responses. *Proc. Natl. Acad. Sci. U. S. A.* **100**:10902–10906.
29. Vence, L., et al. 2007. Circulating tumor antigen-specific regulatory T cells in patients with metastatic melanoma. *Proc. Natl. Acad. Sci. U. S. A.* **104**:20884–20889.
30. Wang, H.Y., et al. 2004. Tumor-specific human CD4+ regulatory T cells and their ligands: implications for immunotherapy. *Immunity.* **20**:107–118.
31. Wang, H.Y., Peng, G., Guo, Z., Shevach, E.M., and Wang, R.F. 2005. Recognition of a new ARTC1 peptide ligand uniquely expressed in tumor cells by antigen-specific CD4+ regulatory T cells. *J. Immunol.* **174**:2661–2670.
32. Beyer, M., and Schultze, J.L. 2006. Regulatory T cells in cancer. *Blood.* **108**:804–811.
33. Fisson, S., et al. 2003. Continuous activation of autoreactive CD4+ CD25+ regulatory T cells in the steady state. *J. Exp. Med.* **198**:737–746.
34. Setiady, Y.Y., et al. 2006. Physiologic self antigens rapidly capacitate autoimmune disease-specific polyclonal CD4+ CD25+ regulatory T cells. *Blood.* **107**:1056–1062.
35. Huehn, J., et al. 2004. Developmental stage, phenotype, and migration distinguish naive- and effector/memory-like CD4+ regulatory T cells. *J. Exp. Med.* **199**:303–313.
36. Kim, J., Rasmussen, J., and Rudensky, A. 2006. Regulatory T cells prevent catastrophic autoimmunity throughout the lifespan of mice. *Nat. Immunol.* **8**:191–197.
37. Bellier, B., Thomas-Vaslin, V., Saron, M.F., and Klatzmann, D. 2003. Turning immunological memory into amnesia by depletion of dividing T

cells. *Proc. Natl. Acad. Sci. U. S. A.* **100**:15017–15022.
38. Marzio, R., Mauel, J., and Betz-Corradin, S. 1999. CD69 and regulation of the immune function. *Immunopharmacol. Immunotoxicol.* **21**:565–582.
39. Podsypanina, K., et al. 2008. Seeding and propagation of untransformed mouse mammary cells in the lung. *Science.* **321**:1841–1844.
40. Madsen, L., et al. 1999. Mice lacking all conventional MHC class II genes. *Proc. Natl. Acad. Sci. U. S. A.* **96**:10338–10343.
41. Lo, D., et al. 1992. Peripheral tolerance to an islet cell-specific hemagglutinin transgene affects both CD4+ and CD8+ T cells. *Eur. J. Immunol.* **22**:1013–1022.
42. Van den Berg, C.L., et al. 1994. Pharmacokinetics of hydroxyurea in nude mice. *Anticancer Drugs.* **5**:573–578.
43. Tough, D.F., and Sprent, J. 1994. Turnover of naive- and memory-phenotype T cells. *J. Exp. Med.* **179**:1127–1135.
44. Fisson, S., et al. 2006. Therapeutic potential of self-antigen-specific CD4+ CD25+ regulatory T cells selected in vitro from a polyclonal repertoire. *Eur. J. Immunol.* **36**:817–827.
45. Billiard, F., et al. 2006. Regulatory and effector T cell activation levels are prime determinants of in vivo immune regulation. *J. Immunol.* **177**:2167–2174.
46. Julia, V., Rassoulzadegan, M., and Glaichenhaus, N. 1996. Resistance to Leishmania major induced by tolerance to a single antigen. *Science.* **274**:421–423.
47. Kleinewietfeld, M., et al. 2005. CCR6 expression defines regulatory effector/memory-like cells within the CD25(+)CD4+ T-cell subset. *Blood.* **105**:2877–2886.
48. Fritzsching, B., et al. 2006. Naive regulatory T cells: a novel subpopulation defined by resistance toward CD95L-mediated cell death. *Blood.* **108**:3371–3378.
49. Seo, N., Hayakawa, S., Takigawa, M., and Tokura, Y. 2001. Interleukin-10 expressed at early tumour sites induces subsequent generation of CD4(+) T-regulatory cells and systemic collapse of antitumour immunity. *Immunology.* **103**:449–457.
50. Setoguchi, R., Hori, S., Takahashi, T., and Sakaguchi, S. 2005. Homeostatic maintenance of natural Foxp3(+) CD25(+) CD4(+) regulatory T cells by interleukin (IL)-2 and induction of autoimmune disease by IL-2 neutralization. *J. Exp. Med.* **201**:723–735.
51. Granucci, F., et al. 2001. Inducible IL-2 production by dendritic cells revealed by global gene expression analysis. *Nat. Immunol.* **2**:882–888.
52. Hanahan, D., and Weinberg, R.A. 2000. The hallmarks of cancer. *Cell.* **100**:57–70.
53. Savage, P.A., et al. 2008. Recognition of a ubiquitous self antigen by prostate cancer-infiltrating CD8+ T lymphocytes. *Science.* **319**:215–220.
54. Kasow, K.A., et al. 2004. Human CD4+CD25+ regulatory T cells share equally complex and comparable repertoires with CD4+CD25- counterparts. *J. Immunol.* **172**:6123–6128.
55. Hsieh, C.S., Zheng, Y., Liang, Y., Fontenot, J.D., and Rudensky, A.Y. 2006. An intersection between the self-reactive regulatory and nonregulatory T cell receptor repertoires. *Nat. Immunol.* **7**:401–410.
56. Shevach, E.M., et al. 2006. The lifestyle of naturally occurring CD4+ CD25+ Foxp3+ regulatory T cells. *Immunol. Rev.* **212**:60–73.
57. Oven, I., et al. 2007. AIRE recruits P-TEFb for transcriptional elongation of target genes in medullary thymic epithelial cells. *Mol. Cell. Biol.* **27**:8815–8823.
58. Aschenbrenner, K., et al. 2007. Selection of Foxp3+ regulatory T cells specific for self antigen expressed and presented by Aire+ medullary thymic epithelial cells. *Nat. Immunol.* **8**:351–358.
59. Savage, P.A., Boniface, J.J., and Davis, M.M. 1999. A kinetic basis for T cell receptor repertoire selection during an immune response. *Immunity.* **10**:485–492.
60. Veiga-Fernandes, H., Walter, U., Bourgeois, C., McLean, A., and Rocha, B. 2000. Response of naive and memory CD8+ T cells to antigen stimulation in vivo. *Nat. Immunol.* **1**:47–53.
61. Klein, L., Khazaie, K., and von Boehmer, H. 2003. In vivo dynamics of antigen-specific regulatory T cells not predicted from behavior in vitro. *Proc. Natl. Acad. Sci. U. S. A.* **100**:8886–8891.
62. Zhou, G., Drake, C.G., and Levitsky, H.I. 2006. Amplification of tumor-specific regulatory T cells following therapeutic cancer vaccines. *Blood.* **107**:628–636.
63. Qin, Z., and Blankenstein, T. 2000. CD4+ T cell–mediated tumor rejection involves inhibition of angiogenesis that is dependent on IFNgamma receptor expression by nonhematopoietic cells. *Immunity.* **12**:677–686.
64. Casares, N., et al. 2003. CD4+/CD25+ regulatory cells inhibit activation of tumor-primed CD4+ T cells with IFN-γ-dependent antiangiogenic activity, as well as long-lasting tumor immunity elicited by peptide vaccination. *J. Immunol.* **171**:5931–5939.
65. Yang, J., et al. 2007. Allograft rejection mediated by memory T cells is resistant to regulation. *Proc. Natl. Acad. Sci. U. S. A.* **104**:19954–19959.
66. Nishikawa, H., Jager, E., Ritter, G., Old, L.J., and Gnjatic, S. 2005. CD4+ CD25+ regulatory T cells control the induction of antigen-specific CD4+ helper T cell responses in cancer patients. *Blood.* **106**:1008–1011.
67. Cederbom, L., Hall, H., and Ivars, F. 2000. CD4+CD25+ regulatory T cells down-regulate co-stimulatory molecules on antigen-presenting cells. *Eur. J. Immunol.* **30**:1538–1543.
68. Dubey, C., Croft, M., and Swain, S.L. 1996. Naive and effector CD4 T cells differ in their requirements for T cell receptor versus costimulatory signals. *J. Immunol.* **157**:3280–3289.
69. Korn, T., et al. 2007. Myelin-specific regulatory T cells accumulate in the CNS but fail to control autoimmune inflammation. *Nat. Med.* **13**:423–431.
70. Galon, J., et al. 2006. Type, density, and location of immune cells within human colorectal tumors predict clinical outcome. *Science.* **313**:1960–1964.
71. Pages, F., et al. 2005. Effector memory T cells, early metastasis, and survival in colorectal cancer. *N. Engl. J. Med.* **353**:2654–2666.
72. Munn, D.H., and Mellor, A.L. 2007. Indoleamine 2,3-dioxygenase and tumor-induced tolerance. *J. Clin. Invest.* **117**:1147–1154.
73. Davis, M.R., Manning, L.S., Whitaker, D., Garlepp, M.J., and Robinson, B.W. 1992. Establishment of a murine model of malignant mesothelioma. *Int. J. Cancer.* **52**:881–886.
74. Marzo, A.L., et al. 1999. Tumor antigens are constitutively presented in the draining lymph nodes. *J. Immunol.* **162**:5838–5845.
75. Gunther, E.J., et al. 2002. A novel doxycycline-inducible system for the transgenic analysis of mammary gland biology. *FASEB J.* **16**:283–292.
76. Darrasse-Jeze, G., Klatzmann, D., Charlotte, F., Salomon, B.L., and Cohen, J.L. 2006. CD4+CD25+ regulatory/suppressor T cells prevent allogeneic fetus rejection in mice. *Immunol. Lett.* **102**:106–109.